Microstructural and Phase Analysis of Zirconium and Copper Binary Thin Film Sputtered by using Elemental Composite Targets†

KONDOH Katsuyoshi*, FUJITA Junji **, UMEDA Junko*, IMAI Hisashi*** and SERIKAWA Tadashi *****

Abstract

Zr-Cu amorphous films were prepared by Radio-Frequency (RF) magnetron sputtering on glass substrates using two kinds of elemental composite targets; Cu chips on Zr plate and Zr chips on Cu plate. It was easy to control precisely the chemical compositions of sputtered films by selecting the chip metal and the number of chips. It is possible to estimate accurately the film compositions by using the sputtered area and the deposition rate of Cu and Zr. XRD analysis on every as-sputtered film showed the broadened pattern. The Zr-rich composition film, however, revealed a small peak at the diffraction angle of $2\theta=35°$, and the Cu-rich one indicated it at $2\theta=43°$. TEM and electron diffraction analysis on the former also showed the main Zr ring patterns and its streaks. When annealing each specimen at 723K in Argon gas, it was found that the former and the latter had a crystallization peak for Zr and Cu at $2\theta=35°$ and 43°, respectively. A Zr-rich composition film with Cu content of 34at% or less showed good corrosion resistance in a salt spray test. On the other hand, a Cu-rich one with 74at% Cu or more was poor. This was because Zr had a higher passivation causing the spontaneous formation of a hard non-reactive surface film that inhibited further corrosion than Cu.

KEY WORDS: (RF-sputtering) (elemental composite target) (Zr-Cu binary film) (crystallization) (corrosion resistance) (standard electrode potential)

1. Introduction

A sputtering process is useful to prepare the amorphous-structured films for use as high-performance materials in industrial fields. The characteristics of films strongly depend on their compositions and structures which are controlled by the sputtering conditions and compositions of target materials. In particular, Zr-Cu alloys are well known as metallic glass materials [1,2], having an obvious glass-liquid transition temperature (Tg), high strength and toughness. In this study, the RF magnetron sputtering process was used to form Zr-Cu amorphous films with various compositions because of its advantages of low-temperature deposition and high controllability in deposition [3,4]. The compositions of sputtered films were estimated by using the deposition rate and sputtered area of each metal in the composite target. The structure of the films was analyzed by XRD, and the crystallization behavior in annealing was evaluated by XRD and TEM observation. The corrosion resistance of Zr-Cu thin films was also investigated in the conventional salt spray test.

2. Experimental

Zr-Cu binary films were deposited by a 13.56 MHz Radio-Frequency (RF) planer-magnetron sputtering. The targets elementally composed of Zr and Cu chips and plates were used in this study. For example, a composite target having 4 pieces of Cu chips on a Zr disk plate is shown in **Fig.1.** Films were deposited on glass substrates placed on the water-cooled substrate holder in the sputtering chamber evacuated to $1.0\text{x}10^{-4}$ Pa pressure. High purity (99.999%) argon gas was used as a sputtering gas at 10 mTorr. The chemical compositions of sputtered films were controlled by changing the number of chips. Before starting the film deposition, pre-sputtering was carried out by placing a shutter-plate between the target and substrate to remove the contaminated surface layer of the target. Sputtering power and sputtering gas pressure were fixed at 150 watts and 10mtorr, respectively. The thickness of the films was about 1μm after 900 s sputtering. The annealing condition was 723K for 900 s in Ar gas atmosphere. X-ray Diffraction (XRD) analysis and Transmission Electron Microscope (TEM) observation were conducted on each sputtered film to investigate the crystallization behavior by annealing. The salt spray test (SST) according to Japan Industrial Standard (JIS) Z 2731 was carried out for 96 hours to evaluate the corrosion resistance.

† Received on December 26, 2008

* Professor
** Graduate Student
*** Specially Appointed Researcher

Transactions of JWRI is published by Joining and Welding Research Institute, Osaka University, Ibaraki, Osaka 567-0047, Japan

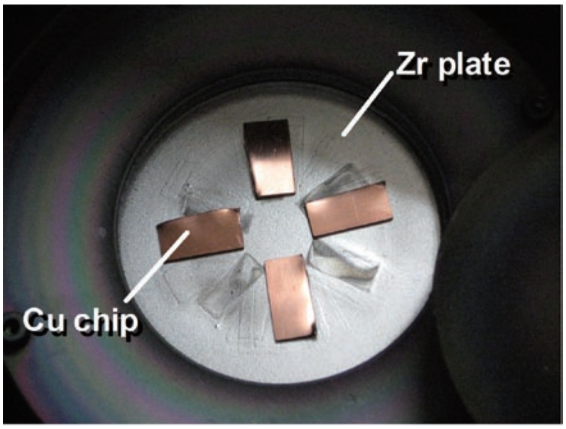

Fig.1 Photograph of elemental composite target used in this study (Cu chips on Zr disk plate).

3. Results

Zr-Cu amorphous thin films with various compositions were deposited by changing the number of Zr or Cu chips on the metal plates. **Figure 2 (a)** shows XRD patterns of the sputtered films, and Cu content for each one was quantitatively measured by Electron Probe Micro-Analysis (EPMA). Basically each shows a broadened pattern indicating an amorphous structure, that is, Zr-Cu binary sputtered films are stably amorphous over a wide range of Cu compositions. In the case of the Cu content of 34 at% or less, however, such Zr-rich films indicate a small peak at 2θ=35°, corresponding to crystallized zirconium as mentioned below. The Cu-rich films with 84at% Cu or more clearly reveal a diffraction peak at 2θ=43°. After annealing each film at 723K for 900s in Ag gas atmosphere, as shown in Fig.2 **(b)**, XRD patterns in Zr or Cu rich composition films clearly reveal crystalline Zr and Cu peaks at 2θ=35° and 43°, respectively. Zr peak intensity gradually increases with increase in Zr content of the film. **Figure 3 (a)** shows a TEM observation of as-sputtered Zr-Cu film with 34at% Cu and its electron diffraction pattern. It basically consists of an amorphous structure. Some spots, however, indicating crystalline Zr, are detected in electron diffraction pattern. It corresponds to a small Zr peak at

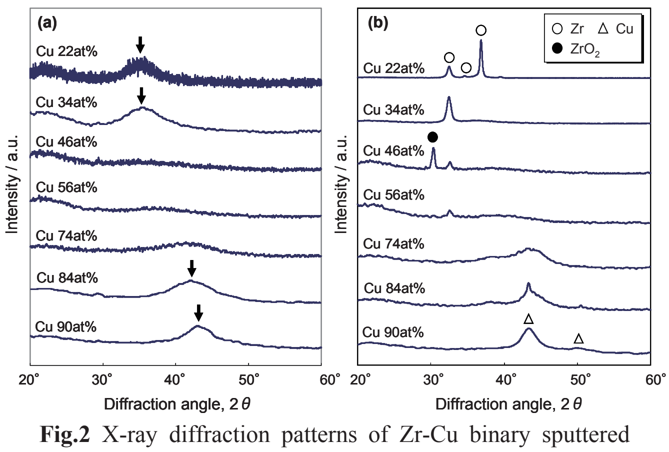

Fig.2 X-ray diffraction patterns of Zr-Cu binary sputtered films with various Cu contents; as-sputtered films (a) and after annealed at 723K for 900s in Ag gas.

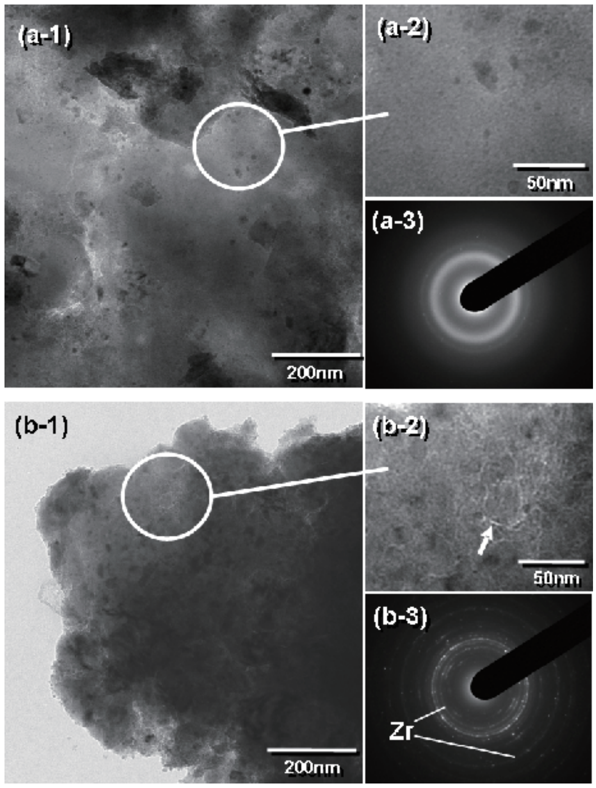

Fig.3 TEM observation of as-sputtered Zr-Cu film with 34at% Cu (a) and after annealed at 1073 K (b).

2θ=35° in Fig.2 (a). A shown in Fig.3 **(b)**, the Zr-Cu sputtered film with 34 at% Cu annealed at 1073K in Ar gas consists of fine Zr crystal grains with 20~40 nm. Accordingly, two kinds of small peaks at 2θ=35° and 43° of as-sputtered films in Fig.2 (a) correspond to the nucleation sites of crystalline Zr and Cu, respectively. They are completely crystallized by annealing at elevated temperature.

The estimation of Zr-Cu film compositions was carried out when changing the number of each chip, and compared to those measured by EPMA. In this study, it is supposed that there is no effect of the contacts between Zr and Cu atoms on each deposition rate in sputtering when employing the elemental composite Zr-Cu target. That is, the composition of Zr-Cu films is determined by both the deposition rate and the sputtered area when using the single metal target. **Figure 4** shows the dependence of Cu composition ratio of each sputtered film measured by EPMA on the number of metal chips of the composite target. It is in proportion to the number of chips when using both Zr and Cu. That is, it is possible to control the sputtered film composition by selecting the metal chip and its number of pieces. Concerning the estimation of the film compositions by using the deposition rate, for example, Cu content of the film (γ_{Cu}) is simply expressed by the sputtered area and deposition rate as shown in equation (1).

$$\gamma_{Cu} = \eta_{Cu} S_{Cu} / (\eta_{Cu} S_{Cu} + \eta_{Zr} S_{Zr}) \qquad (1)$$

where η is a deposition rate and S is a sputtered area.

When considering that the density of the sputtered film is constant, the following equation is obtained.

$$M \times y = \rho \times t \times 10^{-18} \qquad (2)$$

where t; film thickness (μ m), M; atomic mass, y; amount of substance per unit area (mol)

In the equation (2), y value of each metal corresponds to each deposition rate (η), and estimated by measuring the film thickness (t) using each metal target. In this experiment, $y_{Cu} = 3.05\times10^{-13}$ mol and $y_{Zr} = 0.60\times10^{-13}$ mol are obtained when measuring each film thickness of 0.8335 μ m and 2.1767 μ m, respectively. Then, the ratio of each deposition rate ($\alpha = \eta_{Cu} / \eta_{Zr}$) is 5.081. Furthermore, by using this α value, Cu content of the film is calculated by the following equation (3).

$$\gamma_{Cu} = \alpha\beta/(1-\beta+\alpha\beta)$$
$$\beta = S_{Cu}/(S_{Cu}+S_{Zr}) \qquad (3)$$

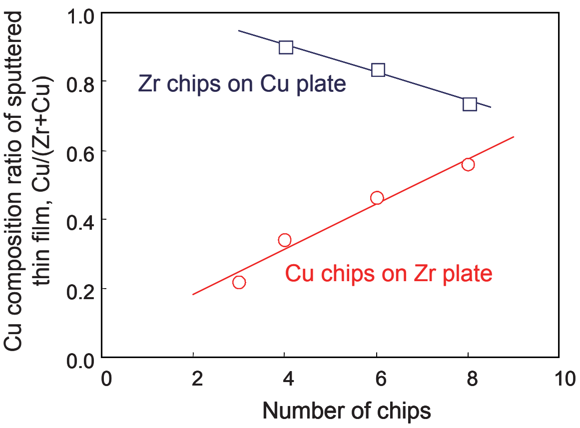

Fig.4 EPMA measurement of Cu composition ratio of films dependence on number of metal chips of elemental composite targets.

Figure 5 indicates a relationship between Cu composition ratio by EPMA and Cu sputtered area ratio (β). When using the composite targets which consist of Zr chips and Cu plate, EPMA measurement corresponds to the calculated values with α=4. The previous study reported that α was 3.9~4.0 when using argon ion sputtering with a reflection ion energy of 100~300eV. Accordingly, the estimation of the film compositions by equation (3) is largely accurate. On the other hand, in the case of the target consisting of Cu chips and Zr plate, the measured Cu content is smaller than that of calculated values with α=4. This is because of the gradual decrease of Cu intensity (○) with increase in the sputtering time as shown in **Fig.6**. The brown color of the as-received Cu chip surface changed into dark brown after discharging for 2.4 ks. The Cu intensity, however, shows a stably constant value (□) in using Zr chips on the Cu plate. EPMA on the dark brown Cu chip specimen indicated that Zr fine particles originated in the target plate covered the chip surface, and caused the reduction of Cu deposition rate in sputtering.

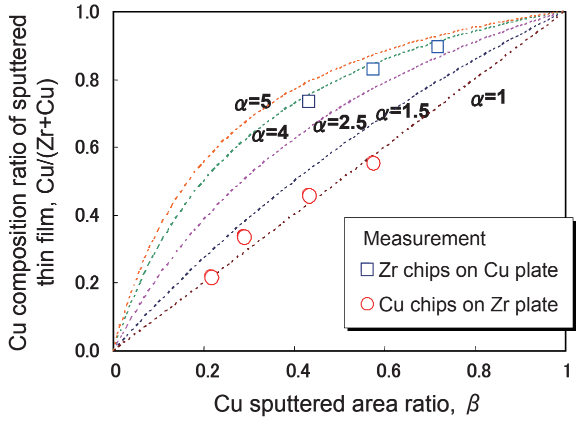

Fig.5 Relationship between Cu composition ratio and Cu sputtered area ratio.

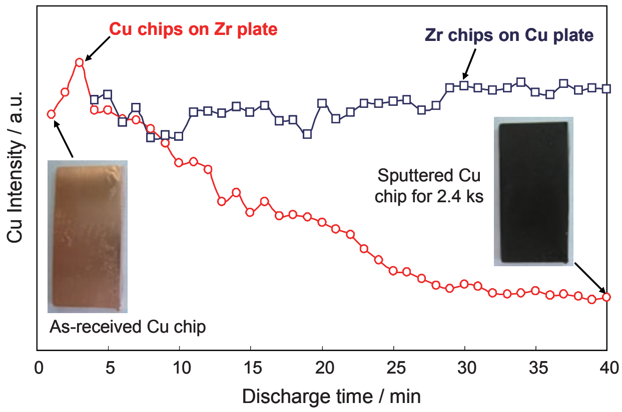

Fig.6 Changes of Cu intensity in spectral diffraction in using Cu chips on Zr plate and Zr chips on Cu plate composite targets.

Figure 7 shows the salt spray test results of as-sputtered films with various Cu contents on the silica glass plate.

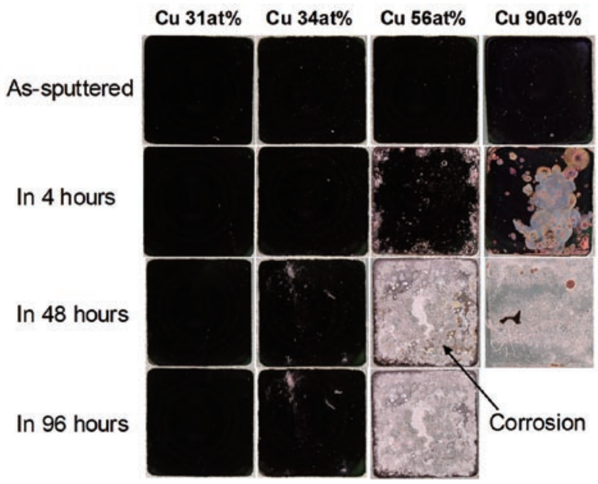

Fig.7 Continuous salt spray test results of as-sputtered Zr-Cu binary films with different content of copper.

The specimens with Cu content of 34 at% or less indicates a good corrosion resistance even after continuously spraying in 96 hours. In the case of 56 at% Cu content, the sputtered film reveals a locally damaged area around the glass plate. This means the corrosion is due to the poor bonding between the film and glass plate. The Zr-rich films with crystallized Zr peaks annealed at 723K also show no corrosion damage after SST for 96 hours. In considering the standard electrode potential of Zr (-1.539 V) and Cu (+0.337 V), the voltage (1.876 V) is effective in accelerating the galvanic corrosion in the crystallized film. However, as mentioned above, this film showed no corrosion damage. It is well known that Zr easily forms passive films in heating under oxidizing atmospheres [5)]. In the SST on the crystallized Zr-rich film after annealing, the passivation due to zirconium oxides causes the control of the corrosion phenomenon. On the other hand, with increase in Cu content of the sputtered films, the poor passivation of Cu is not effective in preventing corrosion damage in SST as shown in Fig.7.

4. Conclusion

The accurate estimation of the sputtered film compositions were carried out by calculating the deposition rate in sputtering and the sputtered area of each metal used in the composite target. In the case of Cu chips on a Zr plate target, the measured Cu contents of the film were smaller than the calculated values because of the reduction of Cu deposition rate due to Zr fine particles covering the Cu chip surface. Every as-sputtered film showed a broadened pattern in XRD analysis. After annealing at 723K, Zr-rich composition film indicated a small peak of crystallized Zr at $2\theta=35°$. Zr-rich films with 34 at% Cu or less had a good corrosion resistance in the SST, and their annealed forms including Zr crystals also showed excellent properties because of the passivation of crystallized zirconium in the film.

References

1) T. Nagase and Y. Umakoshi, Materials Science and Engineering A, 343 (2003) 13-21.
2) Y. K. Kuo, K. M. Sivakumar, C. A. Su, C. N. Ku and S. T. Lin, Physical Review, B74 (2006) 014208.
3) V.S.Veerasamy, H.A.Luten, R.H.Petrmichl, and S.V.Thomsen, Thin Solid Films, 442 (2003) 1-10.
4) P.Fallon, V.S.Veerasamy, C.A.Davis, J.Robertson, G.A.J.Amaratunga, W.I.Milne, and J.Koskinen, Physical Review, B48 (1993) 4777.
5) Corrosion Engineering: Principles and Practice, Pierre R. Roberge, McGraw-Hill (2008), ISBN-10-0071482431.